

Computer simulation on terahertz emission from intrinsic Josephson junctions of high- T_c superconductors

Shizeng Lin,^{1,3} Xiao Hu,¹ and Masashi Tachiki²

¹National Institute for Materials Science, Tsukuba 305-0047, Japan

²Graduate School of Frontier Sciences, The University of Tokyo, Kashiwanoha 277-8568, Japan

³Zhejiang Institute of Modern Physics, Zhejiang University, Hangzhou 310027, People's Republic of China

(Received 21 May 2007; revised manuscript received 6 November 2007; published 15 January 2008)

Solving coupled nonlinear sine-Gordon equations and Maxwell equations numerically, we study the electromagnetic and superconducting properties of the single crystal of high- T_c superconductor $\text{Bi}_2\text{Sr}_2\text{CaCu}_2\text{O}_{8+\delta}$ with a static magnetic field applied parallel to the ab plane and a dc fed in along the c axis. Cavity resonances of transverse plasma occur in the intrinsic Josephson junctions with frequencies in terahertz regime. It is revealed that the electromagnetic wave can transmit from the junctions into space. The emitted energy counted by the Poynting vector is about 400 W/cm^2 . The frequency as well as the energy of emission can be tuned almost continuously by the current and magnetic field.

DOI: [10.1103/PhysRevB.77.014507](https://doi.org/10.1103/PhysRevB.77.014507)

PACS number(s): 74.50.+r, 74.25.Gz, 85.25.Cp

I. INTRODUCTION

Terahertz technology is an extremely attractive field. The main users of the terahertz electromagnetic waves are perhaps the biomedical diagnostics, DNA probe, and cancer detection; a terahertz tomography is also very useful for materials characterization.¹ Although the lower and higher frequency bands of electromagnetic wave can be generated by electronics and photonics, respectively, seeking solid-state, stable generators for the terahertz waves is still a subject of scientific effort. While recently, the semiconductor heterostructures generate terahertz emission with high efficiency,² known as the quantum cascade laser, the issue of frequency tunability has not been resolved.

In the present work, following a previous proposal,³ we seek continuously tunable emission of terahertz electromagnetic wave from high- T_c superconductors with the principle of Josephson relation.⁴ For this purpose, the highly anisotropic high- T_c superconductor $\text{Bi}_2\text{Sr}_2\text{CaCu}_2\text{O}_{8+\delta}$ can be considered as a stack of Josephson junctions in atomic scale.⁵ The device has its advantages since, first, the energy gap in high- T_c superconductors is much larger than the plasma energy and thus the plasma, if excited in some ways, should be stable; second, the power output conjectured to be proportional to the junction number squared would be very large; third, variations of physical parameters in these intrinsic Josephson junctions (IJJs) are much smaller than artificially fabricated junctions. For artificial Josephson junction arrays, radiation of electromagnetic waves has been demonstrated;⁶ the frequency is, however, in the subterahertz regime because of the small superconducting energy gap.

There are theoretical calculations⁷ as well as numerical simulations^{8,9} which discussed possible radiation from IJJs of high- T_c cuprates. However, many issues have not yet been revealed concerning the mechanism of terahertz emission. Although the Josephson plasma obviously plays a key role here, the physical parameters of single Josephson junction of $\text{Bi}_2\text{Sr}_2\text{CaCu}_2\text{O}_{8+\delta}$ only give plasma frequency in subterahertz regime. Therefore, the collective modes in the stack of Josephson junctions are essential in order to lift the frequency

by an order of magnitude. This goal is expected to be achieved by the Josephson vortices driven by the c -axis current, which generates an oscillating voltage across junctions according to the ac Josephson relation. The Josephson plasma and the motion of vortices intervene with each other in a complex way, which makes the resonance condition in this system obscure. Without revealing the resonance mechanism, it is hard to tell whether a continuous tuning of frequency is possible or not.

On the other hand, experimental efforts toward exciting terahertz electromagnetic wave using IJJs seem to be accelerated recently.¹⁰⁻¹² However, there are large discrepancies in estimates of the optimal power output: 3000 W/cm^2 by simulations,⁹ 1500 W/cm^2 by theoretical calculations,⁷ while experimentally, 150 W/cm^2 by Kadowaki *et al.*,¹¹ and 20 W/cm^2 by Bae *et al.*,¹² which hinders a clear assessment on the new technique.

In this study, we investigate the terahertz radiation from intrinsic Josephson junctions by solving coupled nonlinear sine-Gordon equations numerically using an appropriate boundary condition. The strength of the radiation is measured and the frequency spectrum at resonance is obtained. The resonance mechanism and the role of the fluxons are clearly explained based on the numerical results.

II. MODEL EQUATIONS

The model sketched schematically in Fig. 1 is the same as the previous work.⁹ A static magnetic field B_a of order of 1 T is applied along the y axis, which induces Josephson vortices in all insulating layers. A bias current is fed into the system along the z axis, which drives fluxons toward the negative direction of the x axis. The moving fluxons excite the transverse Josephson plasma.^{13,14} For simplicity, we ignore here the effect of thermal fluctuations, and thus, the vortex lines are straight. This approximation reduces the three dimensional system to two dimensions. While the estimate on the output energy should be considered as the upper limit for experiments, the mechanism of radiation remains unchanged even when the thermal fluctuations are involved.

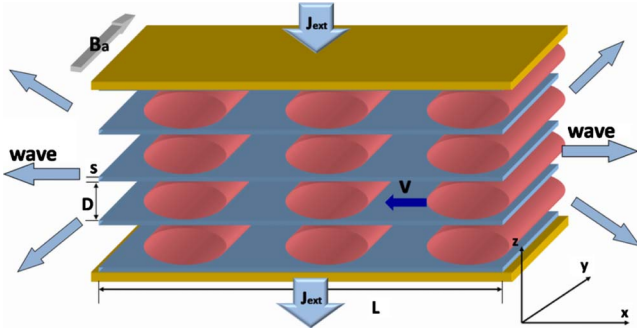


FIG. 1. (Color online) Schematic diagram of the emitter of terahertz electromagnetic wave. The intrinsic Josephson junctions are sandwiched by two gold electrodes through which a dc bias is fed into the system.

Using the London theory, Josephson relation, as well as Maxwell equations, the superconducting and electromagnetic properties of the system can be described by the following equations:^{9,15,16}

$$(1 - \zeta \Delta^{(2)}) \{ \partial_{t'}^2 P_{l+1,l} + \beta \partial_{t'} P_{l+1,l} + \sin P_{l+1,l} + \alpha s' [\partial_{t'} (\rho'_{l+1} - \rho'_l) + \beta (\rho'_{l+1} - \rho'_l)] \} = \partial_{x'}^2 P_{l+1,l}, \quad (1)$$

$$s' (1 - \alpha \Delta^{(2)}) \rho'_l = \partial_{t'} (P_{l+1,l} - P_{l,l-1}), \quad (2)$$

where $P_{l+1,l}$ is the gauge invariant phase difference defined as

$$P_{l+1,l}(\mathbf{r}, t) = \varphi_{l+1}(\mathbf{r}, t) - \varphi_l(\mathbf{r}, t) - \frac{2\pi}{\phi_0} \int_{z_l}^{z_{l+1}} A_z(\mathbf{r}, t) dz, \quad (3)$$

with the phase of order parameter φ , the vector potential A_z , and the quantum flux ϕ_0 . The operator $\Delta^{(2)}$ is defined as $\Delta^{(2)} f_l = f_{l+1} + f_{l-1} - 2f_l$. In Eqs. (1) and (2), dimensionless quantities are used: $x' = x/\lambda_c$, $t' = t\omega_p$, and $\rho'_l = \rho_l \lambda_c \omega_p / J_c$, where ρ_l is the charge density in the l th superconducting layer and $\omega_p = c/\lambda_c \sqrt{\epsilon_c}$ is the plasma frequency, ϵ_c is the dielectric constant along the z axis. Here, λ_c and λ_{ab} in below are the penetration depths. The other dimensionless quantities are defined as $J' = J/J_c$, $B' = 2\pi\lambda_c DB/\phi_0$, $\beta = 4\pi\sigma_c \lambda_c / c \sqrt{\epsilon_c}$, $E' = \sigma_c E / \beta J_c$, $\alpha = \epsilon_c \mu^2 / sD$ (capacitive coupling), $\zeta = \lambda_{ab}^2 / sD$ (inductive coupling), and $s' = s/\lambda_c$, where σ_c is the conductivity, μ is the Debye screening length, J_c is the critical current density, s (D) is the thickness of the superconducting (insulating) layer.

III. BOUNDARY CONDITION

Equations (1) and (2) must be modified at the topmost and bottommost junctions. We assume that the superconductivity will penetrate into the gold electrodes⁹ so that the thickness of the topmost and bottommost superconducting layers s_0 is larger than s . We also assume that the electrodes are good conductor; therefore, the electric field in the electrodes is zero. With these two assumptions, the equations at the topmost and bottommost layers can be written down straightforwardly.¹⁷

The boundary condition at the edges ($x=0$ and $x=L$) is more subtle. We implemented the dynamic boundary condition which is determined by the electromagnetic wave in the dielectric medium coupled to the junctions.^{7,18} Assuming that only the transverse wave is transmitted through the dielectric medium, which becomes exact when the number of junctions is infinite, there is a linear relation between the electric and magnetic fields. With the Fresnel conditions, one arrives at the following condition between the oscillating fields \tilde{B}' and \tilde{E}' on the IJJ side of interface:¹⁸

$$\tilde{B}'^y = \mp \sqrt{\epsilon'_d} \tilde{E}'^z, \quad (4)$$

where $+$ ($-$) means the wave propagating in the negative (positive) x direction and $\epsilon'_d \equiv \epsilon_d / \epsilon_c$ is the dielectric constant of the dielectric medium ϵ_d normalized by ϵ_c . With the relations $\partial_{x'} P_{l+1,l} = B'_{l+1,l}$ and $\partial_{t'} P_{l+1,l} = E'_{l+1,l}$, we derive from Eq. (4) the dynamic boundary condition for the IJJs,

$$\partial_{x'} P_{l+1,l} - B'_a \pm \sqrt{\epsilon'_d} (\partial_{t'} P_{l+1,l} - E'_{dc}) = 0, \quad (5)$$

where the magnetic field induced by J'_{ext} is ignored because it is negligibly small in comparison to B'_a . It is found that $E'_{dc} \approx J'_{ext} / \beta$ in the high-bias region.⁹

The parameters used for simulations are $\lambda_{ab} = 0.4 \mu\text{m}$, $\lambda_c = 200 \mu\text{m}$, $s = 3 \text{ \AA}$, $s_0 = 0.075 \mu\text{m}$, $D = 12 \text{ \AA}$, $\mu = 0.6 \text{ \AA}$, $\alpha = 0.1$, $\beta = 0.02$, and $\epsilon_d = \epsilon_c = 10$. The number of junctions is $N = 30$ and the length $L = 19.2 \mu\text{m}$. The applied magnetic field $B_a = 1 \text{ T}$. The equations of motion, Eqs. (1) and (2), are integrated by the five-point Nordsieck–Gear predictor-corrector method. The time step in all the simulations is set to $\Delta t' = 0.0002$ and the mesh size is set to $\Delta x' = 0.0002$ ($0.1\lambda_{ab}$). We start to calculate physical quantities when the system becomes steady which is identified by the criterion that the voltage oscillates around a fixed value.

IV. NUMERICAL RESULTS

We gradually ramp up the current J'_{ext} at $B_a = 1 \text{ T}$ and then gradually reduce it with the step $\Delta J'_{ext} = 0.01$. The output power is counted by the Poynting vector at the left edge, toward which the vortices are moving. The dependence of the power on the voltage V is plotted in Fig. 2. Strong power emissions take place at discrete values of voltage with equidistance between neighboring peaks. The maximum power is about 400 W/cm^2 .

The spectra of the electric field at the main peaks in Fig. 2 are obtained by the fast Fourier transform and displayed in Fig. 3. The sharp spectra indicate monochromatic electromagnetic waves in *terahertz* regime. Thus, we have confirmed theoretically the terahertz radiation from the intrinsic Josephson junctions.

The equidistance between neighboring peaks indicates a resonance between the Josephson plasma and the cavity modes as revealed below. The Josephson relation reads $\omega_{JP} = 2e\bar{V}/\hbar$ and the cavity modes read $\omega_c = n\pi c_p/L$, where c_p is the velocity of the transverse plasma, \bar{V} is the average voltage across one junction, and n is an integer. The resonance occurs when $\omega_{JP} = \omega_c$, namely,

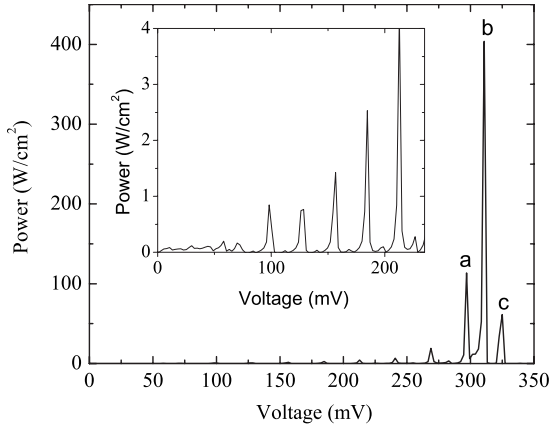


FIG. 2. Radiation power counted by the Poynting vector as a function of the voltage across the stack of IJJs. The external current corresponds to the b peak is $J_{\text{ext}}=1.33J_c$. The inset is the enlarged view of the main panel in the region $V < 235$ mV.

$$\bar{V} \equiv V/N = n\pi\hbar c_p / 2eL. \quad (6)$$

To be more specific, we counted the wavelength λ_w , frequency f , and the voltage \bar{V} at the resonating peaks in Fig. 2, a peak: $\lambda_w=1.82 \mu\text{m}$, $f=4.79$ THz, $\bar{V}=9.90$ mV; b peak: $\lambda_w=1.74 \mu\text{m}$, $f=5.01$ THz, $\bar{V}=10.36$ mV; and c peak: $\lambda_w=1.66 \mu\text{m}$, $f=5.24$ THz, $\bar{V}=10.83$ mV. It is easy to see that $f=2e\bar{V}/h$ and $n\lambda_w/2=L$ for all cases: a peak, $n=21$; b peak, $n=22$; and c peak, $n=23$. The former is nothing but the Josephson relation and the latter is the condition for the cavity modes. From the wavelength and the frequency, we estimate the plasma velocity as $c_p \approx 8.71 \times 10^6$ m/s. It is then easy to see that the interval between consecutive peaks $\Delta\bar{V}=\pi\hbar c_p/2eL=0.47$ mV is satisfied perfectly. Therefore, our simulations indicate clearly that the terahertz radiation is caused by the cavity resonance.

The above plasma velocity c_p is very close to the largest characteristic velocity $c_1=8.75 \times 10^6$ m/s obtained by solving the linearized Eqs. (1) and (2) with $s_0 > s$.¹⁹ The velocity c_1 associated with the nodeless mode is most important for

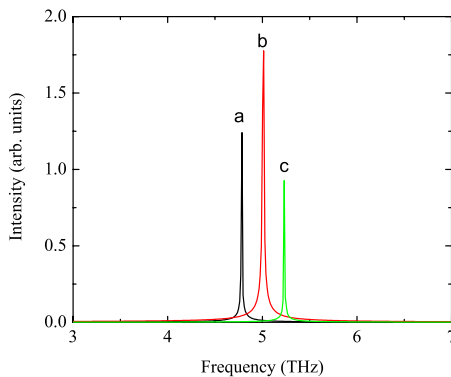


FIG. 3. (Color online) Frequency spectra for the voltage at the main peaks in Fig. 2.

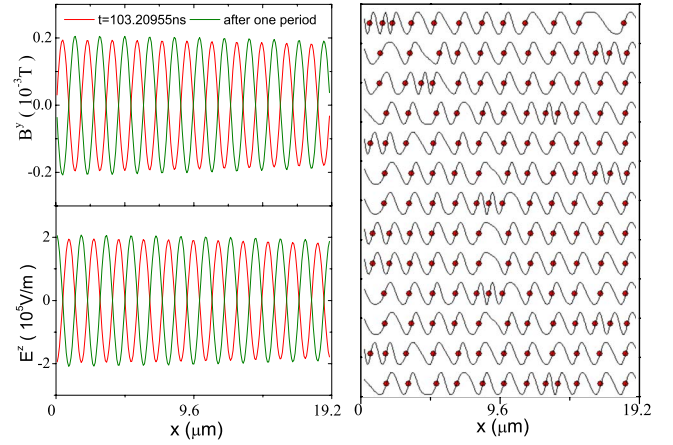


FIG. 4. (Color online) Left panel: snapshots for the magnetic and electric fields at the largest resonance in Fig. 2, where the static backgrounds have been subtracted. Right panel: snapshot of vortex configuration.

resonance since it corresponds to the in-phase motion of vortices.

From Fig. 2, it is clear that there is a bundle of large resonances around $V=310.8$ mV for $B_a=1$ T. In order to reveal the reason for this nonlinear property, we investigate the motion of vortices. Since $P_{l+1,l} = 2\pi DB_a x / \phi_0 + 2\pi c D E_{l+1,l}^z t / \phi_0 + \tilde{P}_{l+1,l}$, where $\tilde{P}_{l+1,l}$ is the small oscillating contribution, the velocity of vortices is evaluated as $v \approx c E_{l+1,l}^z / B_a = 8.63 \times 10^6$ m/s at the b peak in Fig. 2. It is close to the plasma velocities c_p and c_1 . Therefore, the largest resonance takes place when the velocities of vortices and transverse plasma coincide with each other. A similar relation has been discussed by Koshelev and Aranson,²⁰ where an infinitely long junction was considered and therefore no cavity mode was involved.

From $v=c_p=c_1$, it becomes clear that the largest energy emission is excited by a voltage

$$V = N c_1 B_a D / c. \quad (7)$$

With Eqs. (6) and (7), we have $n=2B_a L D / \phi_0$. Since $n\lambda_w/2=L$, it is concluded that the optimal output is achieved when $\lambda_w=\phi_0/B_a D$, namely, the wavelength of plasma equals the vortex-vortex separation.

It is interesting to take a look at the vortex configuration at resonance at this point. As seen from the snapshot shown in Fig. 4, the vortices form an overall ordered rectangular lattice; sliding motions take place in random places for the time being. The rectangular vortex lattice is in accordance with the in-phase plasma velocity.

Having clarified the mechanism of resonance, we turn to investigate how to tune the resonance frequency and power. The voltage dependence of power emission at different magnetic fields is presented in Fig. 5. The voltage generating the largest power output increases linearly with the magnetic field, as described by Eq. (7). From the ac Josephson relation, as depicted in the upper axis of Fig. 5, the frequency of emitted electromagnetic wave can be tuned by sweeping the magnetic field and adjusting the dc voltage accordingly. Al-

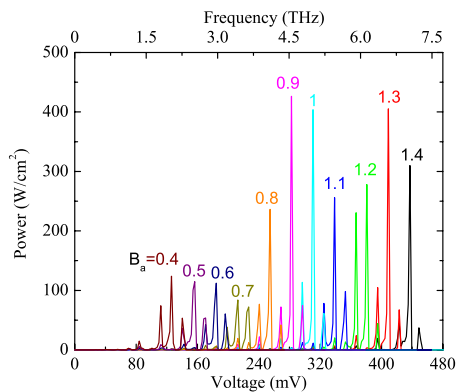


FIG. 5. (Color online) Radiation power at different applied magnetic fields in units of Tesla as a function of the voltage across the stack of IJJs. The frequency in the upper axis is determined by the ac Josephson relation.

though the cavity resonance imposes that the resonating frequency is discrete when voltage is swept, it becomes almost continuous if the length L of IJJs is large enough. For example, the frequency interval between neighboring resonances is about 0.04 THz for $L=100 \mu\text{m}$.

At a given voltage, on the other hand, the emitted power shrinks quickly when the magnetic field is tuned away from the optimal matching value. This permits one to control the power output in a sensitive way.

V. DISCUSSION

We compare briefly our results with recent experimental works. Kadowaki *et al.*¹¹ and Bae *et al.*¹² tried to stimulate terahertz electromagnetic waves utilizing the Josephson vortex dynamics. While the emission was detected by a bolometer in the experiments by Kadowaki *et al.*,¹¹ Bae *et al.*¹² used a second stack of IJJs to detect the excited terahertz electromagnetic waves. It is somewhat difficult to draw conclusions on the resonance mechanism from experiments; in our simulations, however, cavity resonances are clearly revealed. In the experiments by Bae *et al.*,¹² it is found that the most efficient emission is achieved for the rectangular vortex configuration, same as our simulation results. Although not revealing a clear relation, both experiments tried to tune the frequency of emission by sweeping simultaneously the voltage and magnetic field, which, according to our theoretical investigation, is an efficient way for achieving the frequency tunability. In our simulations, we use magnetic fields below

1.5 T, which are quite smaller than those in the experiments.¹² According to the relation for the matching magnetic field and voltage, in order to get large emission power under 4 T, the voltage should be unrealistically large. It can be a possible reason that our theoretical estimate on the power output is different from that in the experiment.

Although singular steps in IV characteristics have been observed in IJJs in several experiments^{21–23} by transport measurements and were explained by the cavity resonance, no direct measurement on the radiation has been reported so far. Our simulations clearly demonstrate strong radiation associated with the cavity modes. Furthermore, the optimal output is achieved when the velocity of fluxons matches the velocity of plasma, which is analogous to the resonance²⁴ of Eck *et al.* in a single junction. We believe that these findings are very instructive for forthcoming experiments.

VI. SUMMARY

To summarize, radiation of terahertz wave occurs at the edges of intrinsic Josephson junctions due to the cavity resonance of the transverse Josephson plasma. A large resonance is achieved when the velocity of Josephson vortices matches the velocity of Josephson plasma. The vortex configuration is revealed to be rectangular with additional random sliding motions at resonance. The maximum output is about 400 W/cm^2 and the frequency covers the terahertz band. Both the energy and frequency can be tuned almost continuously by the bias current and applied magnetic field. Our results show that it is very promising to design generators of terahertz electromagnetic wave based on high- T_c superconductors.

Note added in proof. Recently, we became aware of the latest experimental observation²⁵ on emission of terahertz electromagnetic wave from a single crystal of BSCCO without external magnetic field. The emission is clearly demonstrated in the experiment to be related with the cavity mode of the mesa of BSCCO single crystal, which is consistent with that addressed in the present study.

ACKNOWLEDGMENTS

X.H. acknowledges Q.-H. Chen and Y. Nonomura for discussions at the early stage of this study. Calculations were performed on SR11000 (HITACHI) in NIMS. X.H. is supported by WPI Center for Materials Nanoarchitectonics (MANA), Grant-in-Aid for Scientific Research (C) (No. 18540360) and CTC program of JSPS, CREST-JST, and project ITSNEM of Chinese Academy of Sciences.

¹B. Ferguson and X.-C. Zhang, *Nat. Mater.* **1**, 26 (2002).

²R. Köhler, A. Tredicucci, F. Beltram, H. E. Beere, E. H. Linfield, A. G. Davies, D. A. Ritchie, R. C. Iotti, and F. Rossi, *Nature (London)* **417**, 156 (2002).

³T. Koyama and M. Tachiki, *Solid State Commun.* **96**, 367 (1995).

⁴B. D. Josephson, *Phys. Lett.* **1**, 251 (1962); *Adv. Phys.* **14**, 419

(1965).

⁵R. Kleiner, F. Steinmeyer, G. Kunkel, and P. Müller, *Phys. Rev. Lett.* **68**, 2394 (1992).

⁶P. Barbara, A. B. Cawthorne, S. V. Shitov, and C. J. Lobb, *Phys. Rev. Lett.* **82**, 1963 (1999).

⁷L. N. Bulaevskii and A. E. Koshelev, *J. Supercond. Novel Magn.*

- 19**, 349 (2006).
- ⁸M. Machida, T. Koyama, and M. Tachiki, *Physica C* **362**, 16 (2001).
- ⁹M. Tachiki, M. Iizuka, K. Minami, S. Tejima, and H. Nakamura, *Phys. Rev. B* **71**, 134515 (2005).
- ¹⁰I. E. Batov, X. Y. Jin, S. V. Shitov, Y. Koval, P. Müller, and A. V. Ustinov, *Appl. Phys. Lett.* **88**, 262504 (2006).
- ¹¹K. Kadowaki, I. Kakeya, T. Yamamoto, T. Yamazaki, M. Kohri, and Y. Kubo, *Physica C* **437**, 111 (2006).
- ¹²M.-H. Bae, H.-J. Lee, and J.-H. Choi, *Phys. Rev. Lett.* **98**, 027002 (2007).
- ¹³K. Tamasaku, Y. Nakamura, and S. Uchida, *Phys. Rev. Lett.* **69**, 1455 (1992).
- ¹⁴Y. Matsuda, M. B. Gaifullin, K. Kumagai, K. Kadowaki, and T. Mochiku, *Phys. Rev. Lett.* **75**, 4512 (1995).
- ¹⁵S. Sakai, P. Bodin, and N. F. Pedersen, *J. Appl. Phys.* **73**, 2411 (1993).
- ¹⁶M. Machida, T. Koyama, and M. Tachiki, *Phys. Rev. Lett.* **83**, 4618 (1999).
- ¹⁷T. Koyama and M. Tachiki, *Phys. Rev. B* **54**, 16183 (1996).
- ¹⁸L. N. Bulaevskii and A. E. Koshelev, *Phys. Rev. Lett.* **97**, 267001 (2006).
- ¹⁹S. Sakai, A. V. Ustinov, H. Kohlstedt, A. Petraglia, and N. F. Pedersen, *Phys. Rev. B* **50**, 12905 (1994).
- ²⁰A. E. Koshelev and I. S. Aranson, *Phys. Rev. Lett.* **85**, 3938 (2000); *Phys. Rev. B* **64**, 174508 (2001).
- ²¹A. Irie, Y. Hirai, and G. Oya, *Appl. Phys. Lett.* **72**, 2159 (1998).
- ²²V. M. Krasnov, N. Mros, A. Yurgens, and D. Winkler, *Phys. Rev. B* **59**, 8463 (1999).
- ²³S. M. Kim, H. B. Wang, T. Hatano, S. Urayama, S. Kawakami, M. Nagao, Y. Takano, T. Yamashita, and K. Lee, *Phys. Rev. B* **72**, 140504(R) (2005).
- ²⁴R. E. Eck, D. J. Scalapino, and B. N. Taylor, *Phys. Rev. Lett.* **13**, 15 (1964).
- ²⁵L. Ozyuzer, A. E. Koshelev, C. Kurter, N. Gopalsami, Q. Li, M. Tachiki, K. Kadowaki, T. Yamamoto, H. Minami, H. Yamaguchi, T. Tachiki, K. E. Gray, W.-K. Kwok, and U. Welp, *Science* **318**, 1219 (2007).